Check for updates

Fused aza-heterocyclic ligands: expanding the MOF chemist's toolbox

Oskar G. Wood and Chris S. Hawes [ID] *

Azolate-containing ligands have played an important role in the development of water-stable metal–organic frameworks (MOFs) and related materials due to their particularly strong bonding with earth-abundant first row transition metal ions. Fused ring analogues of pyrazole, imidazole and triazole offer untapped potential to expand the scope of these systems as compact, robust anionic bridging ligands with much greater control over bridging geometries, pendant functionalities and electronic properties. The current design approaches in these systems have been directed by two separate methodologies. In one direction, the simple azoles imidazole, pyrazole and 1,2,4-triazole have been built up by adding fused ring functionality to increase complexity and allow new linker geometries. Meanwhile, in the search for biologically-compatible MOFs, purines such as adenine and hypoxanthine have been explored as linkers and their backbone functionalities optimised to prioritise stability and bridging geometry, leading independently to MOF linkers with similar key features. This highlight article surveys the convergence of these two approaches which both point to the benefits of fused 5–6 ring systems for their electronic and structural properties, and considers the key features that the ideal compact and stable heterocyclic linkers in functional metal–organic frameworks might contain.

Introduction

The explosion of interest in custom-designed microporous materials over the last 20 years has seen metal–organic frameworks (MOFs) leap from structural novelties into a mainstay of materials science.[1] These materials have been studied across all fields of chemistry and have staggering diversity in their structures and compositions, with almost all commercially-available metal ions having been examined as nodes, and linkers reported which span the range of organic and organometallic functionalities at our disposal.[2] Considering that the ligand backbone usually comprises much of the pore surface,[3] and that the nature and strength of the coordination bonding between metal and ligand are key determinants for chemical stability,[4] it is sensible to spend time on careful and deliberate ligand design.

As the proliferation of new MOF structures continues, certain trends have emerged in their design strategies. By far the most successful class of ligands, in terms of both number of MOFs and uptake into pilot-scale projects, has been polycarboxylates.[5] With benzene-1,4-dicarboxylic acid as the archetype, most conceivable combinations of small polyaryl–polycarboxylate ligands have by now been examined as MOF linkers,[6] while

School of Chemical and Physical Sciences, Keele University, Keele ST5 5BG, UK.
E-mail: c.s.hawes@keele.ac.uk

recent advances in aliphatic carboxylates have also seen these systems growing in popularity.[7] Arguably, some of the popularity of carboxylates in these systems may partly result from the necessary crystallographic selection bias for characterisation; crystallisation in these systems is aided by the relatively reversible metal–ligand bonding they exhibit with late first-row d-block metals such as zinc(II).[8] While reliable modulation strategies now exist for crystallising highly stable trivalent and tetravalent metal–carboxylate MOFs,[9] pure carboxylate MOFs with labile divalent nodes tend to suffer from relatively low water stability as a penalty for their reversible formation and crystallisation mechanisms.[10]

Azolate ligands, on the other hand, can show excellent chemical stability with divalent metal ions. Numerous studies with imidazolates, pyrazolates and 1,2,4-triazolates have shown that five-membered nitrogen heterocycles and their derivatives can form highly stable, modular and functional MOFs.[11] For systems of predominantly σ-type coordination bonding, the extra stability shown by azolate complexes towards hydrolysis is easily understood by considering the ca. 10-fold higher pK_a for pyrazole compared to benzoic acid. While very strong metal–pyrazolate bonds can arrest the necessary reversibility in the crystallisation process, to the detriment of crystal quality, pyrazolate and other azolate MOFs also tend to show exceptional stability against hydrolysis.[12] Indeed, the mixed triazolate/oxalate zinc MOF CALF-20 is resilient to humid and acidic gases, and steam

over at least 450 000 adsorption cycles, and has recently been scaled up in a major carbon capture pilot.[13]

Despite the very promising results observed from small azolate ligands in MOF design, much less attention has been paid to their fused-ring analogues, a selection of which are shown in Fig. 1. Commercially-available benzimidazole has seen widespread use in zeolitic imidazolate framework (ZIF) development and as a neutral heterocyclic ligand in various substituted forms,[14] with occasional reports also emerging of the coordination chemistry of aza-benzimidazoles.[15] The benzotriazole motif has also been successfully incorporated as a MOF ligand,[16] with more recent efforts focused on carboxylate-substituted benzotriazoles[17] or fusion of a second 1,2,3-triazolo substituent for MFU-4 type frameworks.[18] However, substituted indazoles are rarely encountered in MOFs, and their higher aza-analogues even less so, with some notable exception of systems derived from adenine and other purine derivatives.[19] Ring fusion of small azolates provides the opportunity not only to temper and finely tune the strength of coordination bonding in these systems, but to access new coordination geometries and backbone functionalities not achievable with traditional carboxylate MOFs. This highlight article outlines the recent developments in designing fused-ring azolate MOF ligands, which lays at the interface of the bottom-up expansion of the pyrazole motif taken by our group and others, and its intersection with the top-down optimisation of bioinspired purine-derived linkers.

Ligand design elements

Structural influences

Of fundamental importance in the design of metallosupramolecular assemblies is careful control over linker geometry.[20] While linker angles close to those associated with the common hybridisation states of their constituent atoms are easily obtained (109.5, 120 and 180° as the geometric sp^3, sp^2 and sp angles, respectively), other bridging angles are more difficult to achieve reliably. Fusion of two or more different sized rings gives access to a range of additional geometries. In a geometrically idealised system, i.e. constructed from the fusion of a regular pentagon (108° internal angle) with a regular hexagon (120° internal angle), if all bond lengths are equal the bridging angles must range from 18–150° (and their complementary values), as shown in Fig. 2. Specific angular geometries of note are the A–C pair, a convenient source of a 90° linker angle in a rigid aromatic system, and 18 and 78° angles from the pairs B–C and B–D, respectively, which do not occur in pure 6-membered ring systems. This expanded range of possible bridging angles has been well used in carbazoles, for example, to give both MOF ligands and anionophores.[21]

Bridging angles in fused systems are susceptible to deformation from bond localization effects and differences in atomic radii when heteroatoms are introduced. Even with only carbon and nitrogen atoms, simple fused aza-heterocycles can exhibit up to 10% variations in bond lengths. For example, 1-aryl-1H-indazoles tend to show bond localisation at the C3 position,[22] favouring C=N and C–C character (e.g., C=N and C–C distances of 1.31 and 1.43 Å, respectively, in 1-(2,4-dinitrophenyl)-1H-indazole).[23] In thiophenes, these deviations become even larger.[24] The influence of heteroatom size and the subsequent subtle deformation of coordinating substituents has been used to great success in the design of both discrete and polymeric systems. The Fujita group have shown size control in metallocapsules can be achieved with even relatively small
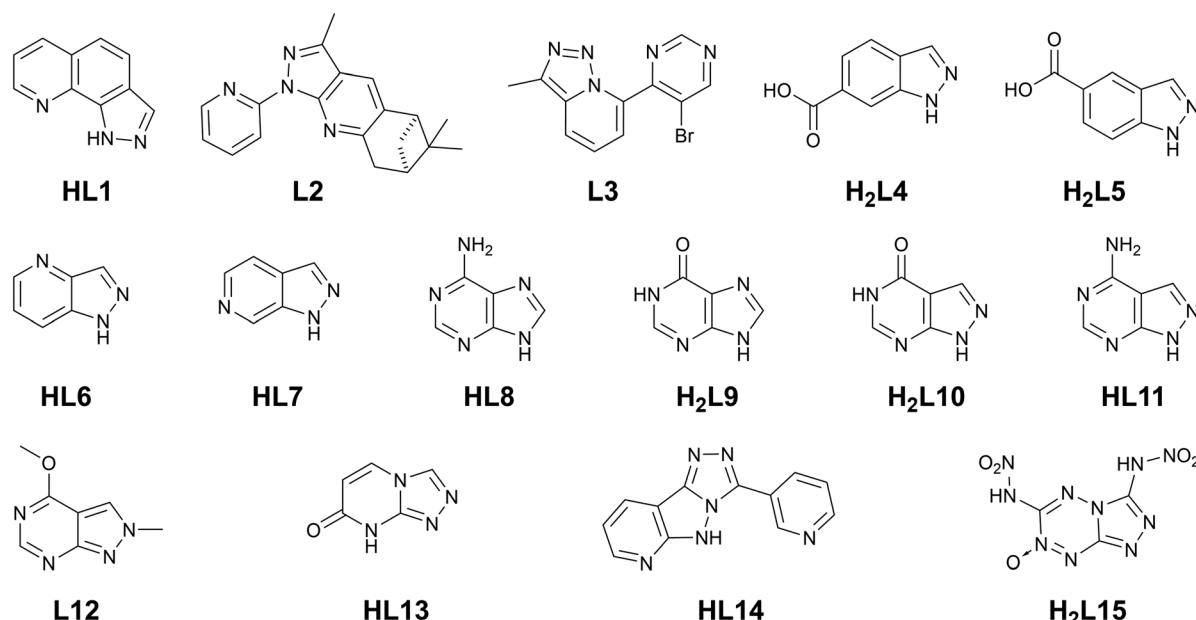
Fig. 1 Ligands of interest to this discussion; each is represented in its neutral (protonated) form.
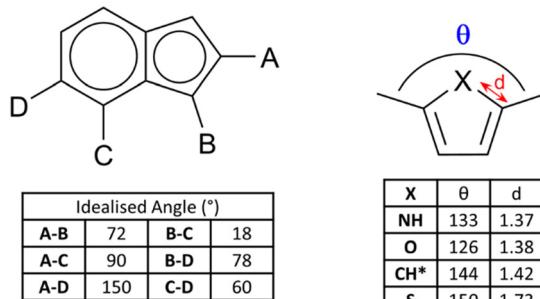
Fig. 2 (Left) Skeletal structure and idealised geometric angles between bond vectors for a generic 6–5 fused ring system with all 10 internal bonds of identical lengths. The angles are derived from geometric relationships between a regular hexagon (internal angles 120°) and a regular pentagon (internal angles 108°). (Right) Examples of deviations in C–X distance and bridging angle for 2,5-disubstituted heterocycles, with data derived from representative crystallographic examples for unbound 2,5-dimethyl derivatives of pyrrole,[27] furan[28] and thiophene.[29] *The CH example is derived from the ruthenium complex of the 1,3-dimethylcyclopentadienyl anion.[30]

Fig. 3 Structure of the zinc(II) metallacycles formed by pyrimidinyl triazolopyridine ligand **L3**, showing the Cl···π-hole contacts between adjacent complexes as orange lines. Zinc atoms coloured grey, chlorine atoms coloured green, bromine atoms coloured brown.

deviations in linker angle induced by replacement of heteroatoms,[25] and Hua and D'Alessandro demonstrated a similar effect in furan, thiophene and selenophene-containing MOF linkers.[26]

Electronic influences

Beyond purely structural considerations, ring fusion and the incorporation of additional heteroatoms is a useful method for tuning the electronic parameters of ligands in metallosupramolecular assemblies. Ring fusion can either raise or lower the pK_a of imidazole and pyrazole depending on the electronic character of the second ring,[31] with subsequent effects on the stability of coordination bonds from the azolate. Precise control of ligand-centred excited state energy levels is also important in ruthenium polypyridyl-type complexes in terms of influencing the energy of the charge transfer transitions,[32] and notably to introduce environment-sensitive probes into these species.[33] In comparison to pure 6-ring species, systems with mixed 5–6 ring azaheterocycles tend to show higher LUMOs than their 6-membered counterparts. The 1H-pyrazolo[4,3-h]quinoline ligand **HL1**, for example, is a heterotopic analogue of the well-known 1,10-phenanthroline.[34] While the fused pyrazole ligand provides additional bridging and hydrogen bonding functionality, a cyclometallated iridium(III) bis-phenylisoquinoline complex containing the **L1** anion also exhibited unusually high electrochemiluminescence efficiency based on the rigidity of the ligand backbone and optimal electronic properties.[35] More recently, Bryleva and co-workers reported a pyrazolo[3,4-b]pyridine derivative with further fusion to α-pinene, to give a tetracyclic ligand **L2** for efficiently sensitized emission in chiral Sm, Eu and Tb complexes.[36] In that case, the energy of the ligand triplet state was particularly well matched to sensitize the Tb^{3+} ion, giving impressive quantum yields of 0.736 and 0.890 in MeCN and the
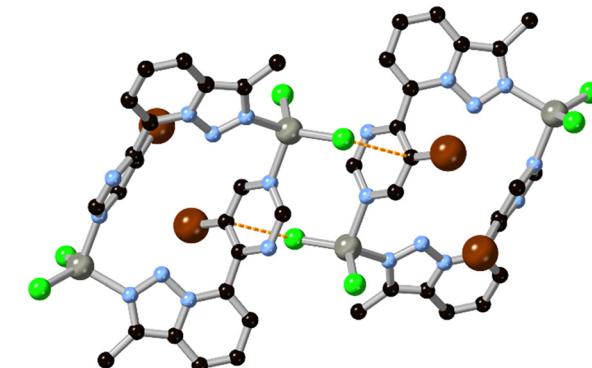
solid state, respectively. Fused rings are a useful source of backbone chirality and a number of camphor-derived chiral fused heterocyclic complexes are known,[37] which include several elegant examples of multinuclear camphor-pyrazole based assemblies.[38] However, the incorporation of this class of chiral backbone into MOFs has not yet been fully explored.

The non-uniform π-electron distribution in nitrogen heterocycles can also be used to good effect in engineering additional structural forces within crystalline assemblies. Recently de Arellano and co-workers reported a M_2L_2 metallomacrocycle formed from the reaction of zinc chloride with the pyrimidinyl triazolopyridine **L3**.[39] Individual metallacycles (containing 90° corners from the triazolopyridine substitution pattern) associate with one another through a novel Cl···π-hole interaction facilitated by the electron deficient bromopyrimidine, as shown in Fig. 3. These interactions lend an additional 5.0 kJ mol^{-1} stabilization energy to the material, which associates into a layered supramolecular structure.

Construction of coordination assemblies and MOFs

Indazoles

One of the simplest fused diazoles, indazole has seen considerably less exploration as a MOF ligand compared to the more common benzimidazole. Various substituted indazoles can be prepared from the corresponding *ortho*-methylanilines, with the divergent 6- and 5-carboxylate derivatives H_2L4 and H_2L5 the most pre-organized for MOF formation.[40] We reported the first example of a MOF containing an indazole linker in 2012 using indazole-5-carboxylic acid H_2L5 which, on coordination to copper(II), gave a twofold-interpenetrated **nbo** network.[41] In that case, with the reaction medium buffered by aqueous ammonium hexafluorosilicate and given the higher pK_a for indazole compared to pyrazole, the ligand coordinates in a mono-anionic bridging mode retaining the N–H proton, as shown in Fig. 4. This group associates with the interpenetrated
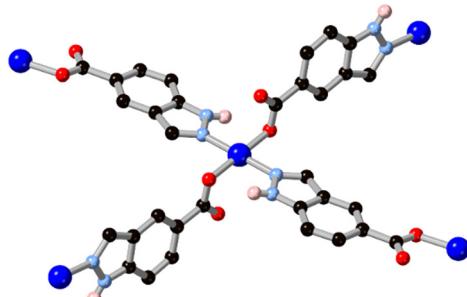
Fig. 4 The coordination environment of the **HL5** anion with copper(II) ions, exhibiting a linear 2-connected coordination geometry with hydrogen bond donor groups proximal to the metal sites. Copper atoms coloured dark blue.

network through N–H⋯OCO hydrogen bonding with a coordinating carboxylate. Despite the coordination sphere containing relatively weakly bound azole (rather than azolate) ligands, the system showed surprisingly high resilience to hydrolysis, being indefinitely stable in neutral water and on exposure to air. Subsequent work with **H₂L4** gave a 2-dimensional polymer with copper(II) ions, though this material was considerably less stable likely due to the presence of copper paddlewheel nodes and persistence of the singly-protonated form of the ligand.[40]

Anionic bridging modes of indazole carboxylic acid derivatives have recently been reported by Rodríguez-Diéguez

and co-workers for **H₂L5**, formed at higher effective pH from the use of metal acetate salts in DMF/H₂O mixtures.[42] As shown in Fig. 5, the bridging 5-carboxyindazolate dianion acts as a 3-connecting bridging ligand, and with further bridging of dinuclear zinc nodes by dipyridyl co-ligands a twofold-interpenetrated **pcu** network is the result. In this species, the dianionic carboxyindazolate ligand acts as an electron donor in a thermochromic ligand–ligand charge transfer (LLCT) process between the high energy azolate orbitals and acceptor orbitals on the dipyridyl co-ligands. Subsequent work has shown versatile coordination behaviour in other indazole-carboxylic acid isomers, although still more commonly coordinating in their monoanionic (N–H) forms.[43]

Introducing additional heterocyclic functionality on the fused six-membered ring gives access to a family of ligands not only with lower pK_a, and thus with more tendency towards *in situ* deprotonation, but also with more compact and geometrically controlled coordination geometries. We recently reported the coordination chemistry of the isomeric pair of ligands pyrazolo[4,3-*b*]pyridine (4-azaindazole) and pyrazolo[3,4-*c*]pyridine (6-azaindazole), **HL6** and **HL7** respectively.[44] On coordination to zinc(II) ions in the presence of a dicarboxylate co-ligand, both azolates display essentially equivalent coordination behaviour, forming two-dimensional zinc–azolate nets which are bridged into 3-dimensional MOFs by the dicarboxylate, represented in Fig. 6. Slight angular variations within the azolate layers perturb the bridging
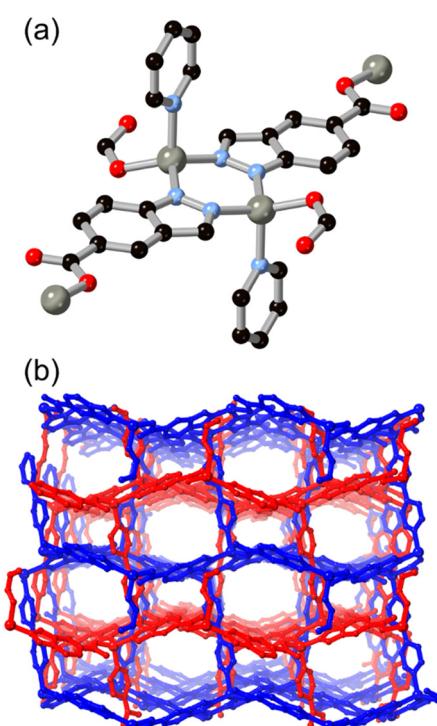

Fig. 5 (a) Coordination of the dianionic **L5** linker to zinc ions in the presence of a dipyridyl co-ligand; (b) extended structure of the resulting MOF showing porosity retained between interpenetrating networks, coloured separately. Zinc atoms coloured grey.
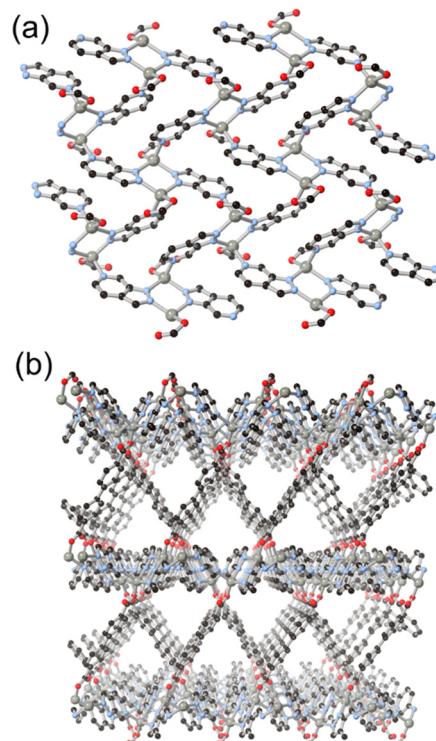
Fig. 6 (a) Structure of the two-dimensional Zn–**L7** network formed in the presence of linking dicarboxylate co-linkers; (b) the extended structure of the ZnL7(bpdc) MOF showing triangular channels between dense zinc–azolate layers. Zinc atoms coloured grey.

angles of the carboxylate linkers, favouring either **rob** or **mab** topologies for the extended structures. In both cases, interpenetration is prohibited by the densely packed two-dimensional metal azolate layers. Despite the presence of coordinatively unsaturated zinc(II) sites within the structures, both materials retain single crystallinity on exposure to air, losing less than 20% of their BET surface areas after one week of ambient exposure. We ascribe this stability to the distribution of anionic character across both ligand types, providing a further electrostatic barrier to each of the possible modes of ligand displacement by water molecules. This feature contrasts with the typical neutral heterocycle/anionic carboxylate pairings more commonly employed in mixed-ligand systems.[45]

Adenine and other purines

Substitution of further heteroatoms into the indazole or benzimidazole skeletons gives purine-type systems which have also seen increasing use in MOF synthesis in recent years, and where the coordination trends seen in indazoles are also evident. While the parent pyrazolopyrimidine and imidazolopyrimidine (purine) skeletons have been studied in coordination compounds in their unsubstituted forms,[46] the amino or oxo derivatives adenine **HL8**, hypoxanthine **H$_2$L9** and allopurinol **H$_2$L10** have proven especially effective as compact polytopic linkers in MOFs. Research in this direction has largely been directed from the biological relevance of these linkers, rather than building up from smaller rings, but the coordination chemistry of these systems shows clear parallels with that seen in the indazole-derived linkers described above.

Of these systems, adenine has been especially important.[47] With up to five coordination sites and a substantially lower pK_a than indazole and benzimidazole for deprotonation at the azole, adenine can act as a potent and compact bridging ligand for high-connectivity systems. With a single negative charge and four heterocyclic coordination sites, adeninate and other purinates can favour the inclusion of polycarboxylate co-ligands for charge balance with 4-coordinate divalent metal ions. BioMOF-1, a zinc(II) MOF with an adenine/4,4′-biphenyl dicarboxylic acid mixed ligand system,[48] was reported by Rosi and co-workers in 2008 and remains a popular platform for guest uptake and exchange studies.[49] The adenine coordination mode in BioMOF-1 occupies each of the core nitrogen atoms in a μ_4 coordination mode, and a high level of water stability is observed in this system. Natarajan and co-workers have also reported a series of coordination polymers containing adenine and aliphatic dicarboxylates with d^{10} metal ions,[50] and observed mixed μ_3 and μ_4 coordination modes in those systems, as shown in Fig. 7. In cases where adenine and other purines retain vacant coordination sites, multidentate hydrogen bonding interactions can act as further structural linkages. Domínguez-Martín and co-workers have also recently showed the metal coordination behaviour of an isomeric adenine
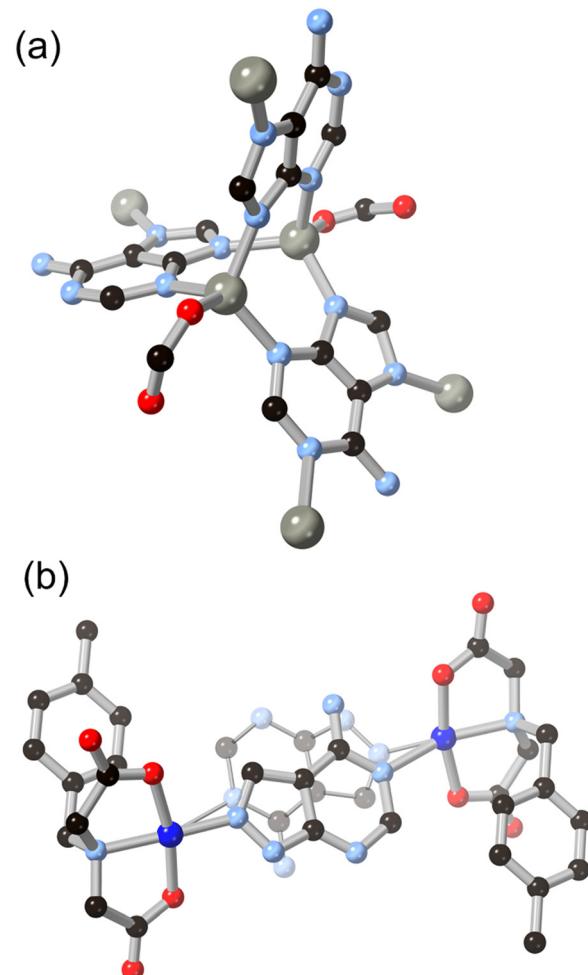
Fig. 7 (a) The mixed coordination modes of adeninate **L8** with zinc(II) ions in the presence of carboxylate co-linkers b) linear bridging mode observed from **H$_2$L11** in a copper(II) complex, two disordered orientations of the ligand species shown as overlapping. Zinc atoms coloured grey, copper atoms coloured dark blue.

species 4-aminopyrazolo[3,4-*d*]pyrimidine **H$_2$L11**,[51] which acts as a near-linear μ_2 bridging ligand when coordinating in its neutral form (Fig. 7).

More recently, hypoxanthine **H$_2$L9** and its isomer allopurinol **H$_2$L10** (Fig. 8) have made appearances as notable heteroaromatic ring systems in MOF development. Cai and co-workers recently reported a hypoxanthine MOF ZnBTCHx containing zinc(II) and a 1,3,5-benzenetricarboxylate co-ligand, with a novel **zyg** topology.[52] Similarly to adenine in BioMOF-1, **H$_2$L9** adopts an anionic μ_4 coordination mode in that system, although due to the similarity in bridging angles of the two rings, crystallographic disorder overlays the imidazole and pyrimidine groups in the structure. Like other mixed-ligand azolates, ZnBTCHx shows excellent resilience to water exposure, so much so that aqueous guest uptake can be performed with tryptophan.

Following the same C/N translocation which relates **HL8** to **HL11** above, the hypoxanthine isomer allopurinol **H$_2$L10** has also been conceived as a MOF linker. Rosi has recently
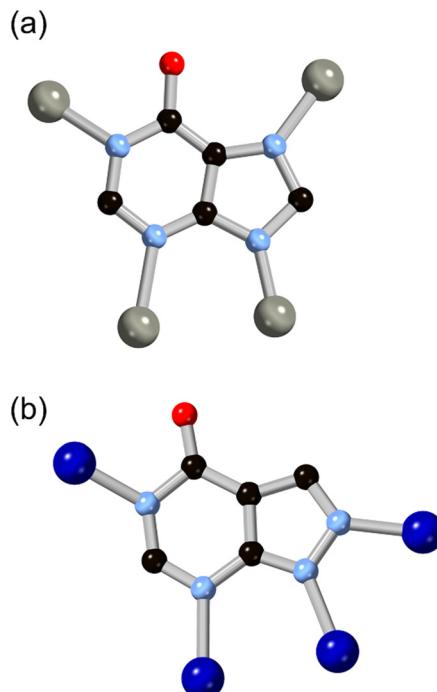
Fig. 8 The structures and μ_4 coordination modes of the **L9** (a) and **L10** (b) dianions with zinc(II) and cobalt(II) ions, respectively. Zinc atoms coloured grey, cobalt atoms coloured dark blue.

Fig. 9 (a) The coordination geometry of the **L10** dianion in ALP-MOF 1 and 2 (zinc(II) and cobalt(II), respectively). (b) Extended structure of ALP-MOF 1 and 2 showing hexagonal channels capable of reversible and well-ordered water uptake. Zinc atoms coloured grey, cobalt atoms coloured dark blue.

reported the structure of ALP-MOFs 1 and 2, mixed allopurinol–terephthalate MOFs with either zinc(II) or cobalt(II) nodes, respectively.[53] In these systems, the orientation of the nitrogen donors in the μ_4 anionic linker allows for the close bridging of three metal ions from the contiguous N–N–C–N edge of the ligand, as shown in Fig. 9. Tetranuclear nodes are supported by two such **L10** ligands, and linked to adjacent clusters by coordination of the distal nitrogen atom and μ_4 terephthalate dianions. Both ALP-MOF-1 and 2, and their mixed-metal analogues, are robust to repeated water uptake and desorption cycles and show remarkable ordering of water clusters within their hexagonal channels.

The metal coordination in ALP-MOF-1 and 2 relates to that previously observed by Zhu with the same allopurinol ligand and 2,5-thiophenedicarboxylic acid as a co-ligand.[54] In that case, a similar threefold-capping of a polynuclear cluster node was observed from the **L10** ligand, but only on a single face with the remaining coordination sites occupied by carboxylate groups. As such, the cluster nuclearity was limited to three zinc ions, with dimethylammonium cations present for charge balance. The resulting MOF, with the unusual **yfy** topology, showed strong affinity for small molecule adsorbates mostly through interactions with the thiophene units. The authors identify C–H···O contacts involving the thiophene carboxylate oxygen atoms when C_2H_2 is adsorbed, but also note a C···S contact for the CO_2 adsorbed system of 3.507 Å which is supported by C–H···O contacts from the thiophene C–H groups (H···O distances

2.5–2.6 Å). Additional surface contacts are observed with the allopurinol ligand; the oxo group participates in an O···C contact with CO_2 at a distance of 3.355 Å while additional contacts with the π surface are less directional.

The tendency for close bridging from the amidine-like fragment in allopurinol and derivatives seems to be maintained even in the absence of a negative charge on the system. When further coordination through the pyrazole ring and deprotonation to the anionic form is blocked in allopurinol derivative **L12** by methylation, the close bridging μ_2 coordination mode is retained in a sodium iodide coordination polymer reported by Bookser and co-workers.[55] In this system, **L12** units alternate between μ_2 and terminal coordination modes with the pyrimidine nitrogen atom either coordinating or accepting chelating hydrogen bonds from nearby aqua ligands. As shown in Fig. 10, the distal pyrimidine nitrogen atom remains non-coordinating, likely due to both the expected weaker coordination to alkali metals and the steric bulk of the adjacent methyl ether.

Fused triazoles and higher nitrogen content systems

The possibilities for further coordination within 5–6 fused ring systems can be expanded by examining triazole and
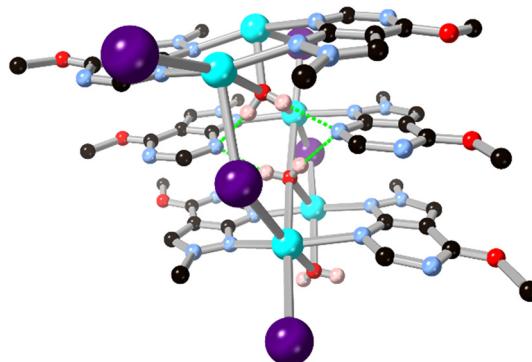
Fig. 10 The coordination geometry of **L12** in its hydrated sodium iodide coordination polymer showing the close μ^2 coordination mode and hydrogen bond accepting character. Sodium atoms coloured cyan, iodine atoms coloured purple, and hydrogen bonds are shown as green dashed lines.
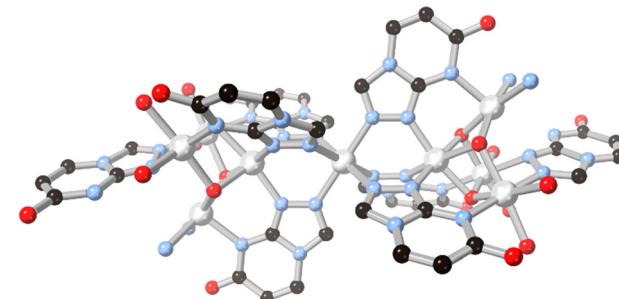
Fig. 11 The μ_3 coordination mode of **L13** anions to nickel(II) ions in the nonanuclear cluster reported by Salameh and co-workers.[59] Nickel atoms coloured light grey.

rings with higher nitrogen content. Simple fused 1,2,4 triazoles such as 1,2,4-triazolo[3,4-*b*]pyridazine have been examined for their coordination chemistry, exemplified by the report by Cingi and co-workers with cadmium(II),[56] although in that case the heterocycle acted only as a monodentate capping ligand. The electronics of the 1,2,3-triazolo[1,5-*a*]pyridine ring system have also been explored by Fitchett and co-workers in discrete mononuclear ruthenium(II) complexes.[57] As with the diazolate cases discussed above, in that system the comparatively electron rich fused ring system tends to increase the HOMO–LUMO separation and leads to blue-shifted MLCT absorbances compared to [Ru(bpy)$_3$]$^{2+}$.

The 7-oxo-1,2,4-triazolo[4,3-*a*]pyrimidine ring system **HL13** provides an interesting comparison to the allopurinol cases, differing by the reorientation of the oxo group and relocation of the second pyrimidine nitrogen into the ring junction. Salameh and co-workers reported a dinuclear silver(I) complex with the neutral form of the ligand, coordinated through the triazole nitrogen atoms only.[58] In the presence of aqueous ammonia, however, full deprotonation of the ligand led to a nonanuclear nickel(II) species capped by six μ_3 and two μ_2 **L13** anions.[59] The coordination in this species draws strong parallels to those observed from **H$_2$L10** and **HL11** in the absence of both a fourth coordination site on the ligand backbone and bridging carboxylate co-ligands. As shown in Fig. 11, two tetranuclear clusters act to orient three **L13** ligands each towards a central octahedral nickel ion, where each tetranuclear moiety can be thought of as a *fac*-tridentate metalloligand. In the absence of fully divergent bridging ligands, the clusters are capped by terminal ammine and aqua ligands, but conceptually the linking of these species into higher dimensionality can be readily envisaged by drawing comparison to the allopurinol systems.

A possible route to expanding the connectivity of these systems lays in further ring fusions, although this approach has been seldom explored by coordination chemists. In one notable example, Li and co-workers found that a

7-azaindazole-type fragment could be further conjugated by fusion with an additional 1,2,4-triazole ring.[60] The resultant tricyclic ligand **HL14**, bearing a pendant 3-pyridyl substituent, was formed in an *in situ* solvothermal cyclisation from 3,5-di(3-pyridyl)-4-amino-1,2,4-triazole in the presence of copper(II) nitrate. Although the resulting coordination polymer, shown in Fig. 12, only showed coordination through three of the five possible nitrogen sites, the novel 5–5–6 fused tricyclic system offers a possible new route to expansion of the binding motifs observed above.

While 1,2,3-triazole and 1,2,4-triazole derivatives tend to exhibit relatively good thermal and mechanical stabilities, increasing the nitrogen content further in fused 5–6 ring systems risks introducing shock sensitivity from highly exothermic decomposition pathways.[61] Nonetheless, where isolation of their metal complexes is possible, some of these energetic materials exhibit fascinating coordination chemistry as high-connectivity linkers.[62] Shreeve and co-workers recently reported a 1,2,4-triazolo[4,3-*b*][1,2,4,5] tetrazine core whose nitramino *N*-oxide derivative **H$_2$L15** acts as a 5-connecting ligand in a coordination polymer with hydrated potassium ions, shown in Fig. 13.[63] In that system
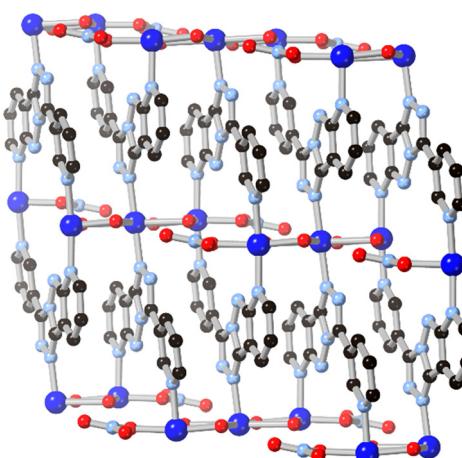
Fig. 12 The extended structure of the copper(II) coordination polymer containing **L14** reported by Li and co-workers.[60] Copper atoms coloured dark blue.
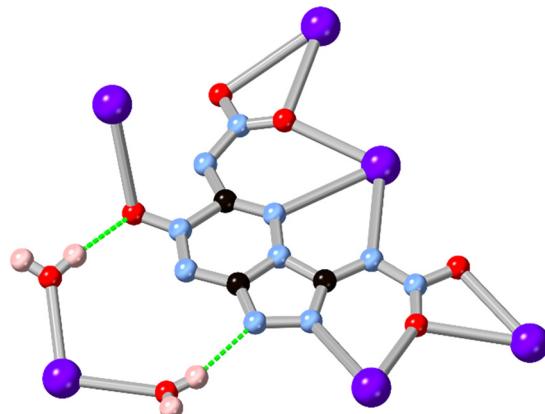
Fig. 13 Coordination environment of the potassium coordination polymer containing **L15** reported by Shreeve and co-workers,[63] exhibiting a μ_5 coordination mode. Potassium atoms coloured light purple, and hydrogen bonds are shown as green dashed lines.

the most prominent coordination occurs through the oxo and nitro groups rather than from the heterocyclic core, unsurprising given both the electronic nature of the cation and the low basicity of the electron deficient core.

Conclusions and outlook

With the goal of enhanced control over metal binding strength, bridging geometry and backbone electronic properties, significant progress in azolate MOFs has been achieved within the last 5 years. New examples of robust, water-stable MOFs containing ample backbone space for further functionalisation and tuning have emerged from ever more complex and information-rich azolate ligands. Both the upwards approach starting from pyrazole and the refinement of more complex purines into their base coordinating elements point towards the broader importance of the 5–6 fused azolate skeleton as a general-purpose building unit for MOFs.

The prevalence of mixed carboxylate–azolate coordination spheres in heterocyclic MOFs has undoubtedly enabled a greater range of structural diversity and opportunities for orthogonal functionality in both ligand types. However, given the typically lower stability of metal–carboxylate bonds compared to homoleptic metal azolates for first-row transition metal ions, a renewed focus on generating homoleptic MOFs with expanded azolate ligands may yield fruit in the search for long term stability in these systems. To do so, fusion of further azolate groups in tricyclic systems may be a useful avenue, alongside exploration of 5–5 fused systems such as pyrazolo[4,3-*c*]pyrazole.[64] In the same way that the purinates and aza-indazolates have proven highly amenable to crystallisation, we suggest that controlling the coordination strength of other fused azolates may be achieved by installation of additional heteroatoms into the ligand backbone or remote electron withdrawing substituents. Backbone chirality is also an avenue worth further pursuing in these systems. Ring fusion provides

opportunities for adding structurally-influential clefts into the ligand backbone. As well as fusion to chiral motifs such as camphor and pinene, bridging of heterocyclic units through elements that add 3-dimensional character to aromatic ligands such as the Tröger's base motif may yield useful chiral structures with the added stability that azolates can provide.[65]

Finally, the need for scalability in ligand synthesis should be recognised as an essential element throughout the design process. Fused azaheterocycles may possess inherent advantages over larger polyaryl–polycarboxylates in scalability by virtue of typically avoiding the need for metal-catalysed coupling steps in their syntheses. However, given the need for MOF production on (at least) the ton to kiloton scale for realistic gas separation applications, it is essential that the next generation of MOF ligands include practical synthetic handles to allow the use of renewable or bio-derived feedstocks.[66] With this in mind, the tolerance to backbone modification shown by purine analogues may prove a significant asset in future materials design.

Conflicts of interest

There are no conflicts to declare.

Acknowledgements

Notes and references

1 R. Robson, *Dalton Trans.*, 2008, 5113–5131; Z. Ji, R. Freund, C. S. Diercks, P. Hirschle, O. M. Yaghi and S. Wuttke, *Adv. Mater.*, 2021, **33**, 2103808; R. Freund, O. Zaremba, G. Arnauts, R. Ameloot, G. Skorupskii, M. Dincă, A. Bavykina, J. Gascon, A. Ejsmont, J. Goscianska, M. Kalmutzki, U. Lächelt, E. Ploetz, C. S. Diercks and S. Wuttke, *Angew. Chem., Int. Ed.*, 2021, **60**, 23975–24001.

2 T.-H. Chen, I. Popov, W. Kaveevivitchai and O. Š. Miljanić, *Chem. Mater.*, 2014, **26**, 4322–4325; C. S. Hawes, *Dalton Trans.*, 2021, **50**, 6034–6049; S. M. Moosavi, A. Nandy, K. M. Jablonka, D. Ongari, J. P. Janet, P. G. Boyd, Y. Lee, B. Smit and H. J. Kulik, *Nat. Commun.*, 2020, **11**, 4068.

3 P. D. C. Dietzel, P. A. Georgiev, M. Frøseth, R. E. Johnsen, H. Fjellvåg and R. Blom, *Chem. – Eur. J.*, 2020, **26**, 13523–13531; Z. Ji, H. Wang, S. Canossa, S. Wuttke and O. M. Yaghi, *Adv. Funct. Mater.*, 2020, **30**, 2000238.

4 S. Yuan, L. Feng, K. Wang, J. Pang, M. Bosch, C. Lollar, Y. Sun, J. Qin, X. Yang, P. Zhang, Q. Wang, L. Zou, Y. Zhang, L. Zhang, Y. Fang, J. Li and H.-C. Zhou, *Adv. Mater.*, 2018, **30**, 1704303.

5 J. Ren, X. Dyosiba, N. M. Musyoka, H. W. Langmi, M. Mathe and S. Liao, *Coord. Chem. Rev.*, 2017, **352**, 187–219; Z. Chen,

M. C. Wasson, R. J. Drout, L. Robison, K. B. Idrees, J. G. Knapp, F. A. Son, X. Zhang, W. Hierse, C. Kühn, S. Marx, B. Hernandez and O. K. Farha, *Faraday Discuss.*, 2021, **225**, 9–69.

6 J. Gu, M. Wen, X. Liang, Z. Shi, M. V. Kirillova and A. M. Kirilov, *Crystals*, 2018, **8**, 83; V. Guillerm and M. Eddaoudi, *Acc. Chem. Res.*, 2021, **54**, 3298–3312.

7 L. K. Macreadie, O. T. Qazvini and R. Babarao, *ACS Appl. Mater. Interfaces*, 2021, **13**, 30885–30890; J. Zhou, T. Ke, F. Steinke, N. Stock, Z. Zhang, Z. Bao, X. He, Q. Ren and Q. Yang, *J. Am. Chem. Soc.*, 2022, **144**, 14322–14329; V. D. Slyusarchuk and C. S. Hawes, *CrystEngComm*, 2022, **24**, 484–490; A. D. Dharma, C. Chen and L. K. Macreadie, *Aust. J. Chem.*, 2022, **75**, 155–159; K. B. Idrees, Z. Chen, X. Zhang, M. R. Mian, R. J. Drout, T. Islamoglu and O. K. Farha, *Chem. Mater.*, 2020, **32**, 3776–3782.

8 R. E. Morris and L. Brammer, *Chem. Soc. Rev.*, 2017, **46**, 5444–5462.

9 G. Wißmann, A. Schaate, S. Lilienthal, I. Bremer, A. M. Schneider and P. Behrens, *Microporous Mesoporous Mater.*, 2012, **152**, 64–70; C. Atzori, G. C. Shearer, L. Maschio, B. Civalleri, F. Bonino, C. Lamberti, S. Svelle, K. P. Lillerud and S. Bordiga, *J. Phys. Chem. C*, 2017, **121**, 9312–9324; G. C. Shearer, S. Chavan, S. Bordiga, S. Svelle, U. Olsbye and K. P. Lillerud, *Chem. Mater.*, 2016, **28**, 3749–3761; J. M. Chin, E. Y. Chen, A. G. Menon, H. Y. Tan, A. T. S. Hor, M. K. Schreyer and J. Xu, *CrystEngComm*, 2013, **15**, 654–657.

10 M. Todaro, G. Buscarino, L. Sciortino, A. Alessi, F. Messina, M. Taddei, M. Ranocchiari, M. Cannas and F. M. Gelardi, *J. Phys. Chem. C*, 2016, **120**, 12879–12889; J. B. DeCoste, G. W. Peterson, H. Jasuja, T. G. Glover, Y.-G. Huang and K. S. Walton, *J. Mater. Chem. A*, 2013, **1**, 5642–5650.

11 S. Menzel, S. Millan, S.-P. Höfert, A. Nuhnen, S. Gökpinar, A. Schmitz and C. Janiak, *Dalton Trans.*, 2020, **49**, 12854–12864; M. R. Bryant, A. D. Burrows, C. M. Fitchett, C. S. Hawes, S. O. Hunter, L. L. Keenan, D. J. Kelly, P. E. Kruger, M. F. Mahon and C. Richardson, *Dalton Trans.*, 2015, **44**, 9269–9280; C. Pettinari, A. Tăbăcaru and S. Galli, *Coord. Chem. Rev.*, 2016, **307**, 1–31; Z. Shi, Y. Tao, J. Wu, C. Zhang, H. He, L. Long, Y. Lee, T. Li and Y.-B. Zhang, *J. Am. Chem. Soc.*, 2020, **142**, 2750–2754; R. Vaidhyanathan, S. S. Iremonger, K. W. Dawson and G. K. H. Shimizu, *Chem. Commun.*, 2009, 5230–5232; C. R. Wade, T. Corrales-Sanchez, T. C. Narayan and M. Dincă, *Energy Environ. Sci.*, 2013, **6**, 2172–2177; H. S. Scott, S. Mukherjee, D. R. Turner, M. I. J. Polson, M. J. Zaworotko and P. E. Kruger, *CrystEngComm*, 2018, **20**, 1193–1197.

12 V. Colombo, S. Galli, H. J. Choi, G. D. Han, A. Maspero, G. Palmisano, N. Masciocchi and J. R. Long, *Chem. Sci.*, 2011, **2**, 1311–1319; T. He, Z. Huang, S. Yuan, X.-L. Lv, X.-J. Kong, X. Zou, H.-C. Zhou and J.-R. Li, *J. Am. Chem. Soc.*, 2020, **142**, 13491–13499; C. Heering, I. Boldog, V. Vesylyeva, J. Sanchiz and C. Janiak, *CrystEngComm*, 2013, **15**, 9757–9768; K. Wang, X.-L. Lv, D. Feng, J. Li, S. Chen, J. Sun, L. Song, Y. Xie, J.-R. Li and H.-C. Zhou, *J. Am. Chem. Soc.*, 2016, **138**, 914–919; S. Mukherjee, N. Sikdar, D. O'Nolan, D. M. Franz, V. Gascón, A. Kumar, N. Kumar, H. S. Scott, D. G. Madden, P. E. Kruger, B. Space and M. J. Zaworotko, *Sci. Adv.*, 2019, **5**, eaax9171.

13 J.-B. Lin, T. T. T. Nguyen, R. Vaidhyanathan, J. Burner, J. M. Taylor, H. Burekova, F. Akhtar, R. K. Mah, O. Ghaffari-Nik, S. Marx, N. Fylstra, S. S. Iremonger, K. W. Dawson, P. Sarkar, P. Hovington, A. Rajendran, T. K. Woo and G. Shimizu, *Science*, 2021, **374**, 1464–1469.

14 T. Xiao and D. Liu, *Mater. Today Energy*, 2019, **14**, 100357; M. B. Lalonde, J. E. Mondloch, P. Deria, A. A. Sarjeant, S. S. Al-Juaid, O. I. Osman, O. K. Farha and J. T. Hupp, *Inorg. Chem.*, 2015, **54**, 7142–7144; Q. Jia, E. Lasseuguette, M. M. Lozinska, M.-C. Ferrari and P. A. Wright, *ACS Appl. Mater. Interfaces*, 2022, **14**, 46615–46626.

15 A. Goswami, D. Ghosh, V. V. Chernyshev, A. Dey, D. Pradhan and K. Biradha, *ACS Appl. Mater. Interfaces*, 2020, **12**, 33679–33689; Y.-Q. Chen, Y. Tian, S.-L. Yao, J. Zhang, R.-Y. Feng, Y.-J. Bian and S.-J. Liu, *Chem. – Asian J.*, 2019, **14**, 4420–4428; H.-W. Wu, L.-W. Lee, P. Thanasekaran, C.-H. Su, Y.-H. Liu, T.-M. Chin and K.-L. Lu, *J. Chin. Chem. Soc.*, 2020, **67**, 2182–2188; A. Dey, D. Bairagi and K. Biradha, *Cryst. Growth Des.*, 2017, **17**, 2885–2892.

16 E. Loukopoulos and G. E. Kostakis, *Coord. Chem. Rev.*, 2019, **395**, 193–229.

17 Q.-Y. Zhang, X. An, L. Xu, J.-H. Yan, S. Zhang, W. Xie and Z.-M. Su, *Inorg. Chem. Commun.*, 2020, **112**, 107726; J.-T. Yuan, J.-J. Hou, X.-L. Liu, Y.-R. Feng and X.-M. Zhang, *Dalton Trans.*, 2020, **49**, 750–756.

18 J. Teufel, H. Oh, M. Hirscher, M. Wahiduzzaman, L. Zhechkov, A. Kuc, T. Heine, D. Denysenko and D. Volkmer, *Adv. Mater.*, 2013, **25**, 635–639; A. M. Wright, Z. Wu, G. Zhang, J. L. Mancuso, R. J. Comito, R. W. Day, C. H. Hendon, J. T. Miller and M. Dincă, *Chem*, 2018, **4**, 2894–2901; R. Röß-Ohlenroth, B. Bredenkötter and D. Volkmer, *Organometallics*, 2019, **38**, 3444–3452.

19 G. Beobide, O. Castillo, A. Luque and S. Pérez-Yáñez, *CrystEngComm*, 2015, **17**, 3051–3059.

20 V. Guillerm, D. Kim, J. F. Eubank, R. Luebke, X. Liu, K. Adil, M. S. Lah and M. Eddaoudi, *Chem. Soc. Rev.*, 2014, **43**, 6141–6172; D. Zhao, D. J. Timmons, D. Yuan and H.-C. Zhou, *Acc. Chem. Res.*, 2011, **44**, 123–133.

21 U. Stoeck, S. Krause, V. Bon, I. Senkovska and S. Kaskel, *Chem. Commun.*, 2012, **48**, 10841–10843; S. Krause, V. Bon, I. Senkovska, U. Stoeck, D. Wallacher, D. M. Többens, S. Zander, R. S. Pillai, G. Maurin, F.-X. Coudert and S. Kaskel, *Nature*, 2016, **532**, 348–352; P. A. Gale, J. R. Hiscock, C. Z. Jie, M. B. Hursthouse and M. E. Light, *Chem. Sci.*, 2010, **1**, 215–220; K. Maslowska-Jarzyna, M. L. Korczak, K. A. Wagner and M. J. Chmielewski, *Molecules*, 2021, **26**, 3205.

22 I. Alkorta and J. Elguero, *J. Mol. Struct.*, 2017, **1137**, 186–192.

23 I. Alkorta, F. P. Cossío, J. Elguero, N. Fresno, L. Hernandez-Folgado, S. García-Granda, L. Menéndez-Taboada, R. Pérez-Fernández, F. Reviriego and L. Vázquez-Viñuela, *New J. Chem.*, 2013, **37**, 2384–2398.

24 W. R. Harshbarger and S. H. Bauer, *Acta Crystallogr., Sect. B: Struct. Sci., Cryst. Eng. Mater.*, 1970, **26**, 1010–1020; C. A. Ramsden, *Tetrahedron*, 2010, **66**, 2695–2699.

25 J. Bunzen, J. Iwasa, P. Bonakdarzadeh, E. Numata, K. Rissanen, S. Sato and M. Fujita, *Angew. Chem., Int. Ed.*, 2012, **51**, 3161–3163.

26 C. Hua and D. M. D'Alessandro, *Cryst. Growth Des.*, 2017, **17**, 6262–6272.

27 R. Schowner, I. Elser, F. Toth, E. Robe, W. Frey and M. R. Buchmeiser, *Chem. – Eur. J.*, 2018, **24**, 13336–13347.

28 T. Ono, Y. Tsukiyama, S. Hatanaka, T. Sakatsume, T. Ogoshi and Y. Hisaeda, *J. Mater. Chem. C*, 2019, **7**, 9726–9734.

29 M. R. Grochowski, W. W. Brennessel and W. D. Jones, *Organometallics*, 2009, **28**, 2661–2667.

30 R. U. Kirss, A. Quazi, C. H. Lake and M. R. Churchill, *Organometallics*, 1993, **12**, 4145–4150.

31 J. Catalan, R. M. Claramunt, J. Elguero, J. Laynez, M. Menendez, F. Anvia, J. H. Quian, M. Taagepera and R. W. Taft, *J. Am. Chem. Soc.*, 1988, **110**, 4105–4111; M. Lõkov, S. Tshepelevitsh, A. Heering, P. F. Plieger, R. Vianello and I. Leito, *Eur. J. Org. Chem.*, 2017, **30**, 4475–4489.

32 M. T. Rupp, N. Shevchenko, G. S. Hanan and D. G. Kurth, *Coord. Chem. Rev.*, 2021, **446**, 214127; J. Romanova, Y. Sadik, M. R. R. Prabhath, J. D. Carey and P. D. Jarowski, *J. Phys. Chem. C*, 2017, **121**, 2333–2343.

33 G. Li, L. Sun, L. Ji and H. Chao, *Dalton Trans.*, 2016, **45**, 13261–13276; A. S. Abel, I. S. Zenkov, A. D. Averin, A. V. Cheprakov, A. G. Bessmertnykh-Lemeune, B. S. Orlinson and I. P. Beletskaya, *ChemPlusChem*, 2019, **84**, 498–503; G. A. Parada, L. A. Fredin, M.-P. Santoni, M. Jäger, R. Lomoth, L. Hammarström, O. Johansson, P. Persson and S. Ott, *Inorg. Chem.*, 2013, **52**, 5128–5137.

34 J. W. Goodwin, P. E. Kruger and C. S. Hawes, *J. Coord. Chem.*, 2021, **74**, 341–360.

35 C.-W. Hsu, E. Longhi, S. Sinn, C. S. Hawes, D. C. Young, P. E. Kruger and L. De Cola, *Chem. – Asian J.*, 2017, **12**, 1649–1658.

36 Y. Bryleva, Y. P. Ustimenko, V. F. Plyusnin, A. V. Mikheilis, A. A. Shubin, L. A. Glinskaya, V. Y. Komarov, A. M. Agafontsev and A. V. Tkachev, *New J. Chem.*, 2021, **45**, 2276–2284.

37 A. A. Warson, D. A. House and P. J. Steel, *Aust. J. Chem.*, 1995, **48**, 1549–1572; A. Petrović, M. M. Milutinović, E. T. Petri, M. Živanović, N. Milivojević, R. Puchta, A. Scheurer, J. Korzekwa, O. R. Klisurić and J. Bogojeski, *Inorg. Chem.*, 2019, **58**, 307–319.

38 M. Sarkar, P. Pandey and J. K. Bera, *Inorg. Chim. Acta*, 2019, **486**, 518–528; M. C. Carrión, I. M. Ortiz, F. A. Jalón, B. R. Manzano, A. M. Rodriguez and J. Elguero, *Cryst. Growth Des.*, 2011, **11**, 1766–1776.

39 C. Ramírez de Arellano, R. Adam, R. Ballesteros-Garrido, B. Abarca, R. Ballesteros, I. Alkorta, J. Elguero and E. Escrivà, *CrystEngComm*, 2020, **22**, 6979–6982.

40 C. S. Hawes and P. E. Kruger, *Dalton Trans.*, 2014, **43**, 16450–16458.

41 C. S. Hawes, R. Babarao, M. R. Hill, K. F. White, B. F. Abrahams and P. E. Kruger, *Chem. Commun.*, 2012, **48**, 11558–11560.

42 A. A. García-Valdivia, M. Pérez-Mendoza, D. Choquesillo-Lazarte, J. Cepeda, B. Fernández, M. Souto, M. González-Tejero, J. A. García, G. M. Espallargas and A. Rodríguez-Diéguez, *Cryst. Growth Des.*, 2020, **20**, 4550–4560.

43 Y.-D. Lan, C.-L. Xiong, C.-X. Huang, W.-M. Xiong and X.-L. Nie, *Z. Kristallogr. - New Cryst. Struct.*, 2021, **236**, 359–361; A. A. García-Valdivia, A. Zabala-Lekuona, G. B. Ramírez-Rodríguez, J. M. Delgado-López, B. Fernández, J. Cepeda and A. Rodríguez-Diéguez, *CrystEngComm*, 2020, **22**, 5086–5095; A. A. García-Valdivia, E. Echenique-Errandonea, G. B. Ramírez-Rodríguez, J. M. Delgado-López, B. Fernández, S. Rojas, J. Cepeda and A. Rodríguez-Diéguez, *Inorganics*, 2021, **9**, 20; W.-F. Zhang, Y. Du, X.-Y. Sun, H.-M. Pan, Y.-Y. Ma, D.-Y. Li, S. Wu, T. Yan and Z.-H. Jing, *Inorg. Chem. Commun.*, 2021, **126**, 108469.

44 A. M. Swarbrook, R. J. Weekes, J. W. Goodwin and C. S. Hawes, *Dalton Trans.*, 2022, **51**, 1056–1069.

45 Z. Yin, Y.-L. Zhou, M.-H. Zeng and M. Kurmoo, *Dalton Trans.*, 2015, **44**, 5258–5275.

46 R. Lyndon, Y. Wang, I. M. Walton, Y. Ma, Y. Liu, Z. Yu, G. Zhu, S. Berens, Y.-S. Chen, S. G. Wang, S. Vasenkov, D. S. Sholl, K. S. Walton, S. H. Pang and R. P. Lively, *Chem. Commun.*, 2022, **58**, 12305–12308; J. Kahr, J. P. S. Mowat, A. M. Z. Slawin, R. E. Morris, D. Fairen-Jimenez and P. A. Wright, *Chem. Commun.*, 2012, **48**, 6690–6692; J. Müller, F.-A. Polonius and R. Roitzsch, *Inorg. Chim. Acta*, 2005, **358**, 1225–1230; W. S. Sheldrick and P. Bell, *Z. Naturforsch., B: J. Chem. Sci.*, 1987, **42**, 195–202.

47 A. Domínguez-Martín, M. del Pilar Brandi-Blanco, A. Matilla-Hernández, H. El Bakkali, V. M. Nurchi, J. M. González-Pérez, A. Castiñeiras and J. Niclós-Gutiérrez, *Coord. Chem. Rev.*, 2013, **257**, 2814–2838.

48 J. An, S. J. Geib and N. L. Rosi, *J. Am. Chem. Soc.*, 2009, **131**, 8376–8377.

49 J. An, C. M. Shade, D. A. Chengelis-Czegan, S. Petoud and N. L. Rosi, *J. Am. Chem. Soc.*, 2011, **133**, 1220–1223; B. N. Bhadra, J. K. Lee, C.-W. Cho and S. H. Jhung, *Chem. Eng. J.*, 2018, **343**, 225–234; A. García-Raso, A. Terrón, Y. Rosseló, A. Frontera, O. Castillo, G. Beobide, S. Pérez-Yáñez, E. C. Escudero-Adán and J. J. Fiol, *CrystEngComm*, 2020, **22**, 4201–4205.

50 S. R. Sushrutha, R. Hota and S. Natarajan, *Eur. J. Inorg. Chem.*, 2016, 2962–2974.

51 A. Domínguez-Martín, D. Choquesillo-Lazarte, J. A. Dobado, H. Martínez-García, L. Lezama, J. M. González-Pérez, A. Castiñeiras and J. Niclós-Gutiérrez, *Inorg. Chem.*, 2013, **52**, 1916–1925.

52 H. Cai, Y.-X. Wu, Z. Lu, D. Luo, J.-X. Sun, G.-W. Wu, M. Li, Y.-B. Wei, L.-M. Zhong and D. Li, *J. Am. Chem. Soc.*, 2022, **144**, 9559–9563.

53 Y. Han, P. Das, Y. He, D. C. Sorescu, K. D. Jordan and N. L. Rosi, *J. Am. Chem. Soc.*, 2022, **144**, 19567–19575.

54 Y.-Z. Li, G.-D. Wang, H.-Y. Yang, L. Hou, Y.-Y. Wang and Z. Zhu, *Chem. – Eur. J.*, 2020, **26**, 16402–16407.

55 B. C. Bookser, M. I. Weinhouse, A. C. Burns, A. N. Valiere, L. J. Valdez, P. Stanczak, J. Na, A. L. Rheingold, C. E. Moore and B. Dyck, *J. Org. Chem.*, 2018, **83**, 6334–6353.

56 M. B. Cingi, A. M. Lanfredi, A. Tirpicchio, J. G. Haasnoot, J. Reedijk, Acta Crystallogr and C. Sect, *Struct. Chem.*, 1986, **42**, 1509–1512.

57 C. M. Fitchett, F. R. Keene, C. Richardson and P. J. Steel, *Inorg. Chem. Commun.*, 2008, **11**, 595–598.

58 S. Salameh, M. Abul-Haj, M. Quirós and J. M. Salas, *Inorg. Chim. Acta*, 2005, **358**, 824–827.

59 S. Salameh, M. Abul-Haj, M. Quirós and J. M. Salas, *Eur. J. Inorg. Chem.*, 2005, 2779–2782.

60 B. Li, D. Jin, B. Ma, D. Liu, G. Li, Z. Shi and S. Feng, *Eur. J. Inorg. Chem.*, 2011, 35–38.

61 M. Kofen, M. Lommel, M. H. H. Wurzenberger, T. M. Klapötke and J. Stierstorfer, *Chem. – Eur. J.*, 2022, **28**, e202200492; B. A. Steele, E. Stavrou, J. C. Crowhurtst, J. M. Zaug, V. B. Prakapenka and I. I. Oleynik, *Chem. Mater.*, 2017, **29**, 735–741.

62 Q. Zhang and J. M. Shreeve, *Angew. Chem., Int. Ed.*, 2014, **53**, 2540–2542; S. Cao, X. Ma, X. Ma, P. Cen, Y. Wu, J. Yang, X. Liu, G. Xie and S. Chen, *Dalton Trans.*, 2020, **49**, 2300–2307.

63 L. Hu, H. Gao and J. M. Shreeve, *J. Mater. Chem. A*, 2020, **8**, 17411–17414.

64 J. Zhang, D. A. Parrish and J. M. Shreeve, *Chem. – Asian J.*, 2014, **9**, 2953–2960.

65 L. Cerrada, J. Cudero, J. Elguero and C. Pardo, *J. Chem. Soc., Chem. Commun.*, 1993, 1713–1714; S. A. Murphy, O. Kotova, S. Comby and T. Gunnlaugsson, *Results Chem.*, 2021, **3**, 100128; J. Cueero, C. Pardo, M. Ramos, E. Gutierrez-Puebla, A. Monge and J. Elguero, *Tetrahedron*, 1997, **53**, 2233–2240; C. S. Hawes, C. M. Fitchett, S. R. Batten and P. E. Kruger, *Inorg. Chim. Acta*, 2012, **389**, 112–117; S. A. Murphy, C. A. Phelan, E. B. Veale, O. Kotova, S. Comby and T. Gunnlaugsson, *Org. Biomol. Chem.*, 2021, **19**, 6817–6833.

66 E.-S. M. El-Sayed and D. Yuan, *Green Chem.*, 2020, **22**, 4082–4104; T. S. Crickmore, H. B. Sana, H. Mitchell, M. Clark and D. Bradshaw, *Chem. Commun.*, 2021, **57**, 10592–10595; P. Marino, P. R. Donnarumma, H. A. Bicalho, V. Quezada-Novoa, H. M. Titi and A. J. Howarth, *ACS Sustainable Chem. Eng.*, 2021, **9**, 16356–16362.